Disease modeling and drug screening for X-linked adrenoleukodystrophy using patient-derived iPS cells

Jae Souk Lee

Department of Medical Science

The Graduate School, Yonsei University

Disease modeling and drug screening for X-linked adrenoleukodystrophy using patient-derived iPS cells

Jae Souk Lee

Department of Medical Science

The Graduate School, Yonsei University

Disease modeling and drug screening for X-linked adrenoleukodystrophy using patient-derived iPS cells

Directed by Professor Dong-Wook Kim

The Doctoral Dissertation
submitted to the Department of Medical Science,
the Graduate School of Yonsei University
in partial fulfillment of the requirements for the degree of
Doctor of Philosophy

Jae Souk Lee

December 2021

This certifies that
the Doctoral Dissertation of
Jae Souk Lee is approved.

Thesis Supervisor:	Dong-Wook Kim
Thesis Committee Member#1:	Joo Young Kim
Thesis Committee Member#2:	Dong-Youn Hwang
Thesis Committee Member#3:	Dae-Sung Kim
Thesis Committee Member#4:	Yong-ho Lee

The Graduate School
Yonsei University

December 2021

Acknowledgements

I would like to express my deepest gratitude to my advisor, Prof. Dong-Wook Kim, for his support throughout my graduate studies. I would also like to extend my appreciation to Prof. Dae-Sung Kim and Prof. Han-Soo Kim for their words of advice, guidance, and encouragement over the years that have made me a better scholar. I would also like to express my sincere gratitude to Dr. Chul-Yong Park for helping me to grow as a person and experience the fundamentals of professional practice.

I would also like to extend a special thanks to Ji Young Kim, Do-Hun Kim, Junwon Lee, Dongjin R. Lee, Jeong-Eun Yoo, Sanghyun Park, Sang-Hwi Choi, and Eunhyun Ji, my laboratory colleagues who inspired me to keep moving forward and stay confident during the demanding and rigorous life of a Ph.D. student. To my friends, Heung Sik Hong, Dong Ik Hwang, Hun Lim, Sejong Lee, Ki Jung Park, and Hui-Wen Liu, I cannot thank you enough for your continuous generosity and friendship.

Finally, I must acknowledge and convey my heartfelt gratitude to my family for their unconditional love.

Table of Contents

List of Figures

LIST OF TABLES

Abstract

Disease modeling and drug screening for X-linked adrenoleukodystrophy using patient-derived iPS cells

Jae Souk Lee

Department of Medical Science
The Graduate School, Yonsei University

(Directed by Professor Dong-Wook Kim)

X-linked adrenoleukodystrophy (X-ALD) is a neurodegenerative disease caused by mutations in the ATP-binding cassette (ABC) transporter subfamily D member 1 (*ABCD1*) gene that encodes the peroxisomal membrane transporter, namely adrenoleukodystrophy protein (ALDP), resulting in the accumulation of very long chain fatty acids (VLCFAs) in organs and serum. Currently, there are no drugs that can cure X-ALD, although Lorenzo's oil has a preventive effect to a certain degree in asymptomatic boys whose brain magnetic resonance imaging is normal. ALDP and three other ABC transporters, namely either adrenoleukodystrophy-related protein (ALDRP, encoded by *ABCD2*), 70-kDa peroxisomal membrane protein (PMP70, encoded by *ABCD3*), and 70-kDa peroxisomal membrane protein-related protein (PMP70R, encoded by *ABCD4*) localized to the peroxisomal

membrane. Interestingly, ALDRP has a functional redundancy with ALDP on the catabolism of VLCFAs. Thus, inducing the over expression of *ABCD2*, the closest homolog of *ABCD1*, has been mentioned as a possible therapeutic option for defective ALDP in X-ALD. Some chemical compounds have been investigated for their ability to induce *ABCD2* expression until now, but none of them have been shown to be effective. In this study, X-ALD iPSCs were generated from X-ALD patient-derived fibroblast for disease modeling and drug screening system was developed for discovery of new drugs. X-ALD iPSCs recapitulated and modeled the pathophysiology of X-ALD disease in terms of abnormal VLCFA accumulation in the iPSC-derived neurons. As a result of drug screening, C5 compound was identified as an upregulator of *ABCD2* promoter activity in X-ALD fibroblasts using a luciferase reporter-based high-throughput screening system. C5 compound reduced VLCFA levels in dose- and time-dependent manners in X-ALD patient-derived cells. These results show that C5 compound has the potential as a therapeutic agent for X-ALD.

Key words: human induced pluripotent stem cells (hiPSCs), X-linked adrenoleukodystrophy (X-ALD), ATP-binding cassette subfamily D member 1 (*ABCD1*), *ABCD2*, very long chain fatty acids (VLCFAs)

Disease modeling and drug screening for X-linked adrenoleukodystrophy using patient-derived iPS cells

Jae Souk Lee

Department of Medical Science
The Graduate School, Yonsei University

(Directed by Professor Dong-Wook Kim)

I. Introduction

Functional gene redundancy is a fundamental aspect of vertebrate evolution.[1,2] Genes within the same gene families, including transcription factors,[3] homeotic genes,[4] signal transduction proteins,[5] and metabolic pathway genes,[6] have been found to have overlapping function. Genes that can completely or partially substitute for each other are candidates for gene therapies for genetic diseases that increase the expression of an endogenous gene rather than introduce a normal copy of the defective gene by transgenesis.

For genetic diseases in humans, X-linked adrenoleukodystrophy (X-ALD) (OMIM, phenotype MIM number 300100) is a disease that may be successfully targeted by such a pharmacological gene therapy. It is caused by a mutation in the ATP-binding cassette transporter subfamily D member 1 (*ABCD1*) gene, which results in defective peroxisomal β-oxidation and the

accumulation of very long chain fatty acids (VLCFAs) with chain lengths of 22-30 carbons.[7-9] It affects mainly central and peripheral myelin, the adrenal cortex, and the testes.[10] X-ALD exhibits highly variable clinical phenotypes. The three main neurological phenotypes are the childhood cerebral form (CCALD), which is characterized by rapid progression, and inflammatory cerebral demyelination in the central nervous system,[11,12] adrenomyeloneuropathy (AMN), which is characterized by slow progression, distal axonopathy in the spinal cord, and peripheral neuropathy; and Addison's disease, which is characterized by adrenal insufficiency without neurologic involvement.[13] The most severe phenotype of X-ALD is CCALD.

ABCD1 is associated with X-ALD. It provides the necessary instructions for producing adrenoleukodystrophy proteins (ALDP) that are located in the peroxisomal membranes. VLCFAs are transported into the peroxisome by ALDP where they are broken down into shorter fatty acid chains. However, *ABCD1* mutation causes VLCFAs to not enter the peroxisome and to accumulate in cells. There are various therapies for this metabolic disturbance of VLCFAs, is to reduce the level of VLCFAs in the cell by inducing *ABCD2* gene expression. This method compensates for ALDP deficiency *in vitro* and *in vivo.*[14-16]

ABCD2 encodes ALDP-related proteins (ALDRP). ALDP and ALDRP may be functionally equivalent given their 88% similarity and 67% identity at the protein level,[17] and the ability of ALDRP to compensate for the biochemical defects found in X-ALD fibroblasts when overexpressed.[15] The two paralogues are usually differentially expressed in a mirror-like pattern, especially in the brain.[18] *ABCD2* can be upregulated by histone deacetylase inhibitors, such as 4-phenylbutyrate (4-PBA),[14,19] valproic acid,[20] suberoylanilide hydroxamic acid,[21] and caffeic acid phenethyl ester,[22] cholesterol depletion via sterol regulatory element-binding protein,[23] fenofibrate[24,25] via peroxisome proliferator-activated receptor α activation,[25]

liver X receptor antagonists,[26] by thyroid hormones[27] and thyromimetics;[28,29] and by Metformin via AMP-activated protein kinase (AMPK) α1.[30] However, many of these drug candidates did not show clear effects in either animal model or clinical trials. CCALD, cyclophosphamide, IFN-β1, thalidomide, cyclosporin, mitoxantrone, natalizumab, and intravenous immunoglobulin administration all failed to produce results.[31-35] Therefore, currently there is no effective treatment for symptomatic X-ALD patients.

Hematopoietic stem cell transplantation (HSCT) is currently the only effective treatment for CCALD patients, but only if it is performed at the early stage of cerebral demyelination.[11] Early results of clinical trials of Lenti-D gene therapy with autologous HSCT have been reported as a safe and effective alternative to allogeneic HSCT.[36] Due to the failure of all other candidate drugs and limited cell transplantation methods, the emerging drug development method is disease modeling and drug screening using induced pluripotent stem cell (iPSC) made from patients' somatic cells.

Generating iPSCs from somatic cells demonstrated that adult mammalian cells can be reprogrammed into a pluripotent state by forcing the expression of a few embryonic transcription factors, namely Oct-3/4, SOX2, KLF4, and c-Myc.[37] The discovery of iPSCs has opened up unprecedented opportunities in the pharmaceutical industry, clinics and laboratories. In addition, the number of medical applications of human iPSCs in disease modeling, drug screening and stem cell therapy has been increasing rapidly.[38] In this study, I generated iPSCs derived from X-ALD patients' fibroblasts and differentiated them into neural cells for disease modeling. Then I performed drug screening on this in vitro disease model to identify drugs for treating X-ALD.

II. Materials and Methods

1. Reagents

A LOPAC 1280 library of pharmacologically active compounds (Sigma-Aldrich, St. Louis, MO, USA) was used to screen for *ABCD2* expression induction. Lovastatin, 4-phenylbutyrate (4-PBA) and C5 compound were also purchased from Sigma-Aldrich. A dual-luciferase reporter assay system was purchased from Promega (Madison, WI, USA).

2. Human fibroblast cultures

Human dermal fibroblasts (HDF; C0045C, Thermofisher Scientific, Waltham, MA, USA) were cultured in Dulbecco's modified Eagle's medium (DMEM; Thermofisher Scientific) supplemented with 10% FBS (Geminibio Products, West Sacramento, CA, USA) and 1% penicillin/streptomycin (P/S; Thermofisher Scientific). Human X-ALD fibroblasts from a single patient with CCALD and AMN (CCALD type; GM04496, AMN type; GM17819, Coriell Institute, Camden, NJ, USA) were cultured in Eagle's minimum essential medium (MEM; Thermofisher Scientific) supplemented with 15% FBS and 1% P/S.

3. Human iPSC generation

Episomal vectors encoding defined reprogramming factors were used as previously described.[39] In brief, X-ALD fibroblasts were grown in MEM supplemented with 15% FBS and electroporated using a Neon microporator system (Thermofisher Scientific) with 3 μg of episomal vector mixtures according to the manufacturer's instructions. After being pulsed three times with a voltage of 1,650 V for 10 ms, the cells were grown in MEM containing 15% FBS. Seven days after transfection, cells were transferred onto a feeder layer of mitomycin-C-treated STO cells (ATCC, Manassas,

VA, USA). iPSC colonies that looked similar to human embryonic stem cells (hESC) were picked up mechanically and further cultured for characterization.

4. Human iPSC cultures

Episomal vector-derived human wild-type iPSCs,[39] and human X-ALD iPSCs were maintained in hESC medium composed of DMEM/F12 (Thermofisher Scientific) medium supplemented with 20% knockout serum replacement (Thermofisher Scientific), 4.5 g/L L-glutamine (Thermofisher Scientific), 1% nonessential amino acids (Thermofisher Scientific), 0.1 mM 2-mercaptoethanol (Thermofisher Scientific), and 4 ng/mL basic fibroblast growth factor (bFGF; PeproTech, Rocky Hill, NJ, USA) as previousely described,[40] In the feeder free condition, iPSCs were maintained in culture dishes coated with Matrigel (Corning, Corning, NY, USA) in STEMMACS iPSC-brew FX (Miltenyi Biotec, Bergisch Gladbach, Germany) medium instead of hESC medium.

5. Differentiation into three germ layers

To test whether iPSCs would differentiate into three germ layers in vitro, embryoid bodies (EB) were formed by partial dissociation and cultured in DMEM/F12 (1:1) medium supplemented with 20% knockout serum, 4.5 g/L L-glutamine, 1% NEAA, 0.1 mM 2-mercaptoethanol, and 15% FBS. Seven days after induction, the EBs were attached to Matrigel-coated culture dishes and further cultured for 14 days. The spontaneous differentiation of EBs into the three germ layer lineages was detected by immunostaining with appropriate antibodies (Table 1).

Table 1. Antibodies used in immunocytochemistry analysis

Antibody	Dilution	Company, Cat. #

Rabbit anti-OCT4	1:200	Santa Cruz, Dallas, TX, USA, Cat. # SC-9081
Rabbit anti-SOX2	1:200	Sigma-Aldrich, Cat. # AB5603
Goat anti-NANOG	1:50	R&D systems, Minneapolis, MN, USA, Cat. # AF1997
Mouse anti-SSEA4	1:200	Sigma-Aldrich, Cat. # MAB4304
Mouse anti-TRA-1-81	1:100	Sigma-Aldrich, Cat. # MAB4381
Mouse anti-TRA-1-60	1:100	Sigma-Aldrich, Cat. # MAB4360
Rabbit anti-NESTIN	1:1000	Sigma-Aldrich, Cat. # ABD69
Goat anti-SOX17	1:200	Santa Cruz, Cat. # SC-17356
Mouse anti-α-SMA	1:400	Sigma-Aldrich, Cat. # A5228
Goat anti-OLIG2	1:200	R&D systems, Cat. # AF2418
Mouse anti-NKX2.2	1:200	DSHB, Iowa City, IA, USA, Cat. # 745A5
Mouse anti-A2B5	1:200	Millipore, Cat. # MAB312
Rabbit anti-NG2	1:200	Millipore,

Rabbit anti- PDGF receptor alpha	1:200	Cat. # AB5320 Abcam, Cambridge, UK, Cat. # AB61219
Mouse anti-SOX10	1:200	R&D systems, Cat. # MAB2864
Mouse anti-O4		R&D systems, Cat. # MAB1326
Rat anti-MBP	1:200	Abcam, Cat. # AB7349
Donkey anti-rabbit IgG (H + L) highly cross-adsorbed secondary antibody, Alexa Fluor 488	1:500	Thermofisher Scientific, Cat. # A-21206
Donkey anti-goat IgG (H + L) cross-adsorbed secondary antibody, Alexa Fluor 488	1:500	Thermofisher Scientific, Cat. # A-11055
Donkey anti-mouse IgG (H + L) highly cross-adsorbed secondary antibody, Alexa Fluor 488	1:500	Thermofisher Scientific, Cat. # A-21202
Donkey anti-mouse IgG (H + L) highly cross-adsorbed secondary antibody, Alexa Fluor 594	1:500	Thermofisher Scientific, Cat. #A-21203
Donkey anti-goat IgG (H + L) cross-adsorbed secondary antibody, Alexa Fluor 594	1:500	Thermofisher Scientific, Cat. # A-11058
Donkey anti-rabbit IgG (H + L) highly cross-adsorbed secondary antibody, Alexa Fluor 594	1:500	Thermofisher Scientific, Cat. #A-21207

6. iPSC differentiation into oligodendrocytes and neurons

iPSCs were differentiated into oligodendrocytes as previously described.[41] iPSC colonies were detached by collagenase type IV (Worthington, Columbus, OH, USA) and EBs were formed by incubation without bFGF in hESC medium supplemented with dorsomorphin and SB431542.[42] After four days, the EBs were plated onto Matrigel-coated culture dishes in DMEM/F12 medium that included N2 supplements (1x; Invitrogen, Carlsbad, CA, USA) and 20 ng/ml bFGF to select and expand neural precursor cells (NPC). After five days, neural rosette structures were mechanically isolated and suspension-cultured with 10 ng/ml bFGF to make spherical neural masses (SNM). The SNMs were passaged to expand the NPCs. The SNMs were then replated onto Matrigel-coated culture dishes and differentiated into oligodendrocyte precursor cells (OPCs) in N2 medium containing 10 ng/ml bFGF and 10 ng/ml epidermal growth factor (EGF; Peprotech, Rocky Hill, NJ) for four-eight days. Then the OPCs were further grown in N2 medium supplemented with 10 ng/ml bFGF and 10 ng/ml platelet-derived growth factor (PDGF; PeproTech) for eight days. Terminal differentiation of oligodendrocytes was then induced by withdrawing the growth factors and adding 30 ng/ml 3,3',5'-triiodo-L-thyronine (T3; Sigma-Aldrich) for three-four weeks.

NPCs were differentiated into neurons by mechanically detaching the cell neural rosette structures, mildly triturating them, plating them onto Matrigel-coated culture dishes, and then culturing them in a differentiation medium composed of DMEM/F12 supplemented with N2, B27, 20 ng/ml glial cell line-derived neurotrophic factor (GDNF; PeproTech), 20 ng/ml brainderived neurotrophic factor (BDNF; PeproTech), 2 ng/ml transforming growth factor β 3 (TGFβ; PeproTech), 200 μM ascorbic acid (Sigma-Aldrich), and 5 μM forskolin (Sigma-Aldrich).

7. Plasmids and reporter gene constructs

The construct pGL3-h*ABCD2* (-800)-Luc is a plasmid that contains the upstream 800 bp region of the *ABCD2* promoter and that was previously described in an earlier report.[43] In order to generate the pGL3-h*ABCD2* (-800x2)-Luc plasmid that contains two copies of the upstream 800 bp region of the *ABCD2* promoter, an additional -800 bp fragment was amplified from human dermal fibroblast genomic DNA as a template and polymerase chain reaction (PCR) products were subcloned onto the Xho I site of the pGL3-h*ABCD2* (-800)-Luc vector. The reporter construct sequences were verified by DNA sequencing (Solgent, Seoul, South Korea).

8. Chemical screening and luciferase reporter assay

A total of 3 x 10^6 CCALD fibroblasts were transiently transfected with 4 μg of ph*ABCD2* (-800x2)-Luc plasmid and 1 μg of pRL-Simian virus (SV40) plasmid (Promega) containing the *Renilla* luciferase gene under the control of the SV40 promoter using a Neon microporator transfection system (Thermofisher Scientific) as previously described.[43] Transfected cells were seeded into 96-well plates and grown for 24 hr. Then, each compound from the library plates was treated at a final concentration of 10 μM for primary screening. A day after treatment, cells were assayed for measurements of firefly and *Renilla* luciferase activities. Luminescence signals were measured using a microplate luminometer (Berthold Technologies, Germany). *Renilla* luciferase activity was used for normalization.

9. RNA isolation and semi-quantitative PCR and quantitative (real-time) PCR

Total RNA was extracted using an Easy-Spin Total RNA Purification Kit (iNtRON Biotechnology, Seoul, South Korea). Then 1 μg of RNA was converted into cDNA with PrimeScript RT Master Mix (Takara Bio Inc.,

Otsu, Japan). Semi-quantitative PCR was performed with the 2x EmeraldAmp GT PCR Master Mix (Takara Bio Inc.) and 10 pmol of each primer. Amplified transcripts were normalized to the glyceraldehyde 3-phosphate dehydrogenase (*GAPDH*)-specific signal. Quantitative (real-time) PCR was performed using TB Green Premix Ex Taq (Takara Bio Inc.) and the CFX96 Real-Time System (Bio-Rad, Hercules, CA, USA). *GAPDH* was used as an endogenous reference to calculate Ct values and relative expression levels ($2^{-\Delta\Delta Ct}$) of target genes. The primer sequences are listed in Table 2.

Table 2. PCR primer sequences

Gene	Primer sequence	Tm (℃)
EBNA-1	F: 5'-ATGGACGAGGACGGGGAAGA -3' R: 5'-GCCAATGCAACTTGGACGTT -3'	58
OCT4	F: 5'-CCTCACTTCACTGCACTGTA-3' R: 5'-CAGGTTTTCTTTCCCTAGCT-3'	64
LIN28	F: 5'-AGCCATATGGTAGCCTCATGTCCG-3' R: 5'-TCAATTCTGTGCCTCCGGGAGCAG-3'	64
NANOG	F: 5'-TGAACCTCAGCTACAAACAG-3' R: 5'-TGGTGGTAGGAAGAGTAAAG-3'	64
REX1	F: 5'-TCACAGTCCAGCAGGTGTTTG-3' R: 5'-TCTTGTCTTTGCCCGTTTCT-3'	64
SOX2	F: 5'-TTCACATGTCCCAGCACTACCAGA-3' R: 5'-TCACATGTGTGAGAGGGGCAGTGTGC-3'	64
TET1	F: 5'-CTGCAGCTGTCTTGATCGAGTTAT-3' R: 5'-CCTTCTTTACCGGTGTACACTACT-3'	64
ABCD2	F: 5'-GAACTGCTGTCATTCAAGAATCTG-3'	64

	R: 5'-TGCCAATGTGTCACTGAGAGG-3'	
GAPDH	F: 5'-CCCCTCAAGGGCATCCTGGGCTA-3' R: 5'-GAGGTCCACCACCCTGTTGCTGTA-3'	64

10. Immunocytochemistry

Cells were fixed with 4% paraformaldehyde in phosphate-buffered saline (PBS) for 15 min, washed with PBS, and permeabilized with PBS containing 0.1% Triton X-100 for 10 min at room temperature. Then, the samples were incubated with blocking buffer, which was PBS containing 3% bovine serum albumin for 1 hr. Then the cells were incubated with primary antibodies diluted in blocking buffer at 4℃ overnight. The next day, the samples were washed three times with PBS and then incubated with fluorescence-tagged secondary antibodies (Table 1) in blocking buffer for 30 min at room temperature.[44] The cover-slips were washed three times with PBS and mounted onto slides using DAPI mounting medium (Vector Laboratories, Burlingame, CA, USA). All images were obtained with an IX71 microscope equipped with a DP71 digital camera (Olympus, Tokyo, Japan).

11. VLCFA analysis

X-ALD fibroblasts were harvested by trypsinization, and the cell pellet was dissolved in PBS. VLCFA analysis was performed by Seoul Clinical Laboratories (Seoul, South Korea) as described previously.[45] VLCFAs were determined by methyl ester formation.[46] Heptacosanoic acid (C27:0) was added as the internal standard to each sample. Then methylene chloride in methanol and acetyl chloride were added and the samples were heated for 4 hr at 85˚C to allow the formation of methyl esters. After cooling, potassium carbonate solution was added to quench the reaction by neutralization. The resulting fatty acid methyl esters were extracted with hexane solution,

followed by extraction with acetonitrile to remove polar compounds. The hexane layer was taken and evaporated to dryness under a gentle stream of nitrogen. The dry residue was reconstituted in hexane for gas chromatography analysis.

12. MTT assay

Cells were seeded into 96 well microplates at a density of $1x10^4$ cells/well and incubated with 1, 3, and 6 μM of C5 compound for 1, 2, and 3 days at 37˚C in an atmosphere containing 5% CO_2. Following incubation with the test compound, the medium was removed and the cells were incubated with 5 μl 3-(4,5-dimethylthiazol-2-yl)-2,5-diphenyltetrazolium bromide (MTT) solution, which was composed of 5 mg/ml MTT in PBS for 1 hr and then solubilized in dimethyl sulfoxide. The amount of purple formazan dye that viable cells produced by converting it from MTT was quantified by measuring absorbance at a wavelength of 540 nm.

13. Karyotyping

G-banding karyotype analysis was performed at passage 25 by GenDix, Inc. (Seoul, South Korea) using standard protocols for GTG banding. A total of 20 metaphases were analyzed at a 550 band resolution.

14. STR analysis

Short tandem repeat (STR) assays were performed by Cosmogenetech Co, Ltd. (Seoul, South Korea). The target loci were amplified using a PowerPlex 18D System Kit (Promega) and analyzed with ABI3130xl genetic analyzer (Applied Biosystems, Waltham, MA, USA) using the software program GeneMapper v.5.0 (Applied Biosystems).

15. Statistical analysis

Data is presented as mean ± SEM. The statistical tests were paired, two-tailed Student *t*-tests, and statistical significance was set at * $p < 0.05$ as compared with DMSO-treated samples.

III. Results

1. Generation of X-ALD specific hiPSCs from CCALD patient-derived fibroblasts

X-ALD is caused by a mutation in *ABCD1* which results in a defect in peroxisomal β-oxidation, which in turn causes the accumulation of VLCFAs.[7-9] In this study, iPSCs were generated from a CCALD patient for disease modeling and drug screening. CCALD patient-derived fibroblasts were reprogramed into iPSCs using integration-free episomal plasmids expressing five pluripotency factors, namely OCT4, SOX2, KLF4, L-MYC, and LIN28. After iPSC production, several iPSC colonies with morphologies similar to those of normal hESCs (Fig. 1A). Their remaining episomal vectors were checked by semi-quantitative PCR with episomal plasmid-specific primers and episomal plasmids were not detected (Fig. 1B). The expression levels of pluripotency markers in CCALD iPSCs were similar to those in H9 human embryonic stem cells (Fig. 1C). The expressions levels of several of the pluripotency markers in protein levels were checked by immunocytochemistry. The pluripotency markers NANOG, OCT4, and SOX2 and the surface markers TRA-1-60, SSEA4, and TRA-1-81 were detected (Fig. 2). CCALD iPSCs had a normal 46XY karyotype (Fig. 3A). STR analysis was performed on genomic DNA extracted from CCALD iPSCs and parental fibroblasts. All 18 STR loci were exact matches with parental fibroblasts (Fig. 3B), which means that the cell line was not contaminated by any other human cell lines and was genetically identical to its parental fibroblasts. Pluripotency was further evaluated by differentiation into three germ layers. EB formation assay detected the expression of the ectodermal marker NESTIN, the endodermal marker SOX17, and the mesodermal marker α-SMA, which indicates that the CCALD iPSCs differentiated into the principal cells in three germ layers (Fig. 4).

Collectively, these results indicate that the CCALD iPSCs differentiated from patient-derived fibroblasts had hESC characteristics and pluripotency.

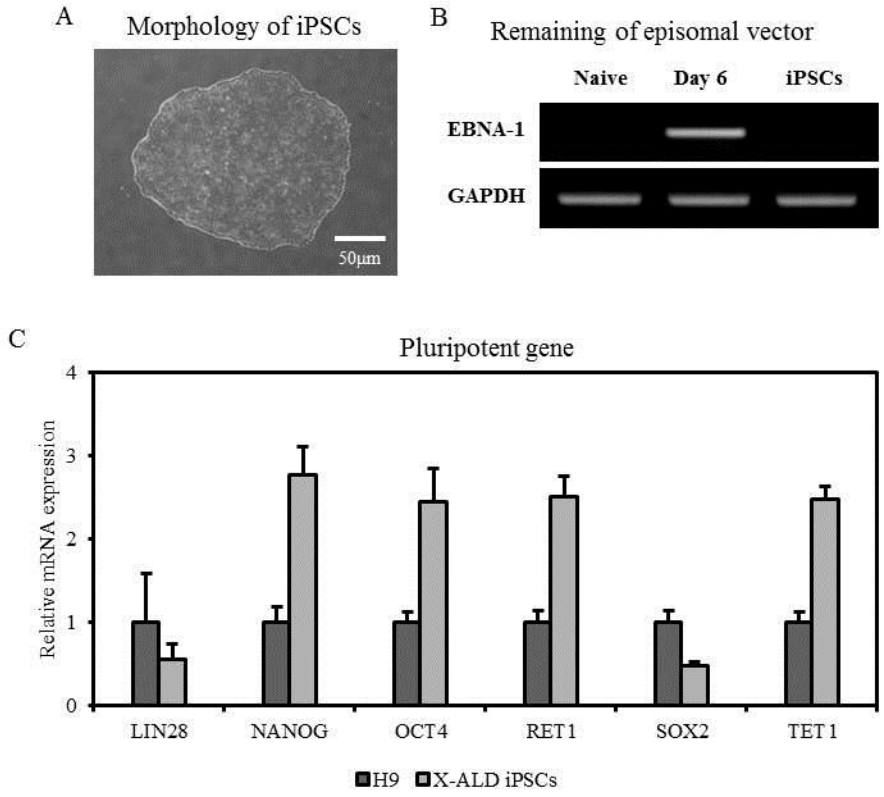

Figure 1. iPSCs generated from CCALD patient-derived fibroblasts. (A) Phase-contrast microscopy showed that X-ALD iPSCs maintained the typical morphology of undifferentiated iPSCs. (B) Semi-quantitative PCR confirmed that episomal plasmids remained in X-ALD iPSCs. (C) The gene expression of pluripotency markers in X-ALD iPSCs, H9 human embryonic stem cells as determined by real-time PCR analysis. Data is given as mean ± SEM. Scale bar = 50 μm.

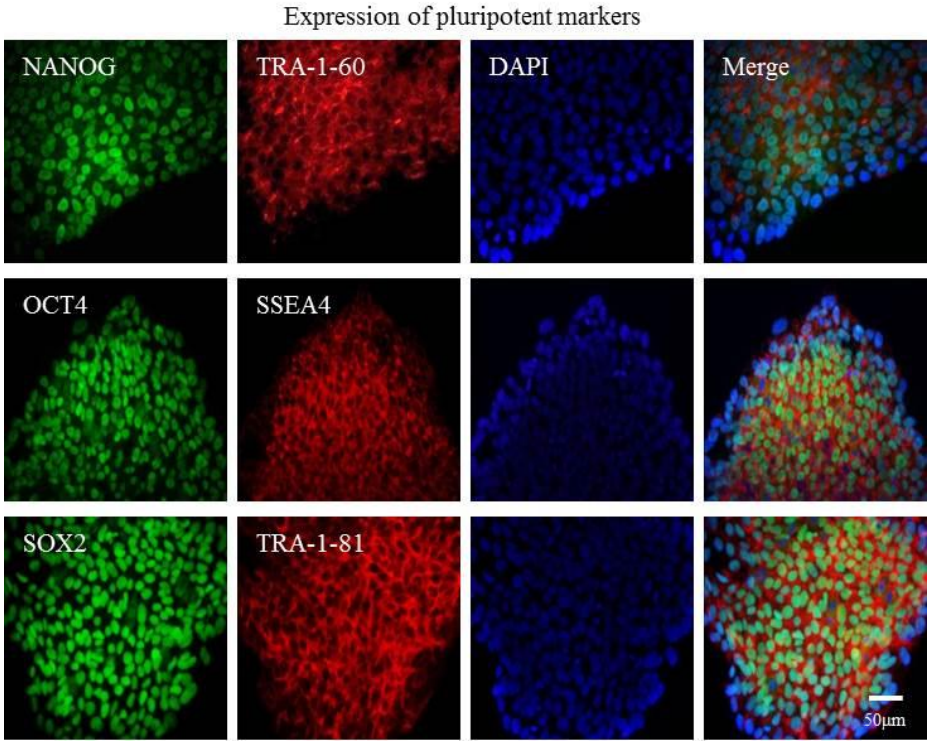

Figure 2. The expression of pluripotency markers was identified by immunocytochemistry. X-ALD iPSC colonies expressed the pluripotency markers NANOG, OCT4, and SOX2 and the surface markers TRA-1-60, SSEA4, and TRA-1-81. Scale bar = 50 μm.

A

Karyotype

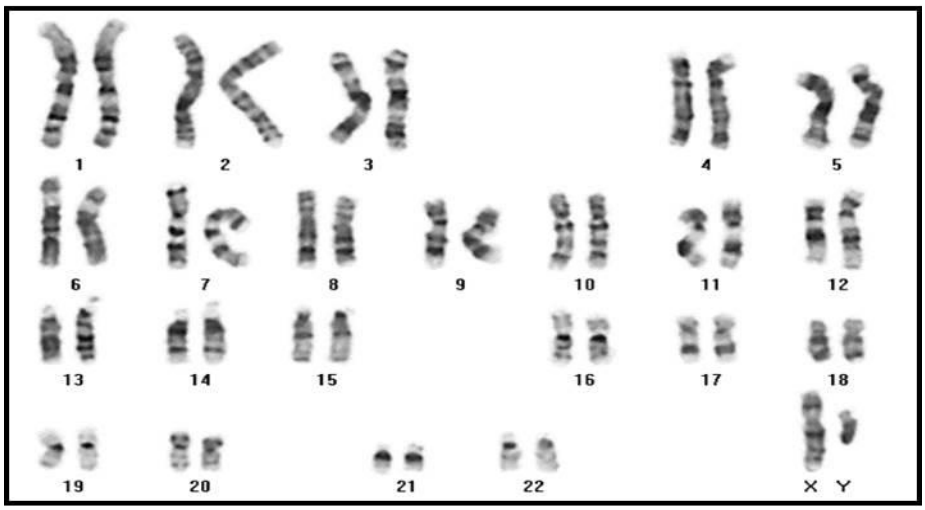

B

STR analysis

Locus	Reference Database Profile Database : ALD Fibroblast		Sample Profile Sample Name : ALD iPSC		Shared alleles #
D5S818	11	12	11	12	2
D13S317	9	11	9	11	2
D7S820	8	10	8	10	2
D16S539	10	11	10	11	2
vWA	15		15		1
TH01	6	9.3	6	9.3	2
TPOX	8		8		1
CSF1PO	11	13	11	13	2
AMEL	X	Y	X	Y	2
D3S1358	15		15		1
D21S11	30	31.2	30	31.2	2
D18S51	16	19	16	19	2
D8S1179	10	13	10	13	2
FGA	19	21	19	21	2
D2S1338	16	20	16	20	2
D19S433	13	15	13	15	2
Penta D	9		9		1
Penta E	15	16	15	16	2
Number of shared alleles					32
Total number of alleles in the reference database profile					32
% match					100.0%
Result interpretation					**Related**

Figure 3. Results of karyotype and STR analyses of iPSCs derived from CCALD patient-derived fibroblasts. (A) Results of G-banding analysis of iPSCs' human karyotype. (B) STR analysis results of the CCALD iPSCs and parental CCALD fibroblasts genes.

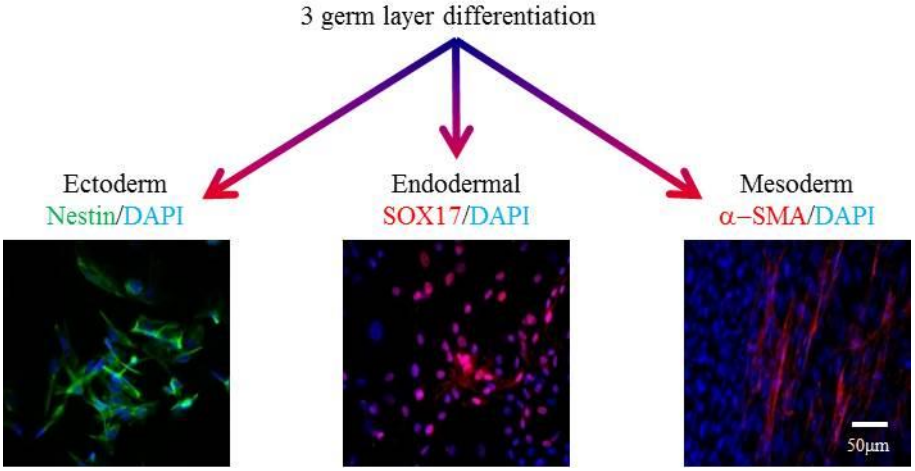

Figure 4. Differentiation of CCALD iPSCs into derivatives of three germ layers. Immunochemistry showed that the three germ layer markers, namely α-SMA for the mesoderm, NESTIN for the ectoderm, and SOX17 for the endoderm were expressed. Scale bar = 50 μm.

2. iPSC differentiation into oligodendrocyte

Oligodendrocytes (OLs) are one of the types of cells strongly affected in X-ALD patients. To determine whether deleting *ABCD1* affects oligodendrocyte differentiation, oligodendrocytes were generated from wild type (WT), CCALD, and AMN iPSCs according to established protocols.[41] EBs were cultured with dorsomorphin and SB431542 for 4 days and were then attached to Matrigel-coated dishes. After 5 days, these cultures had preferentially generated neural rosette structures. The SNMs that were formed from these neural rosette structures were used to expand NPCs. Then the SNMs were plated onto Matrigel-coated dishes and cultured in the

presence of EGF and PDGF for 2 weeks to differentiate them into oligodendrocyte precursor cells (OPCs). Immunocytochemistry with OLIG2, NKX2.2, A2B5, NG2, SOX10 and PDGF receptor alpha antibodies revealed that the OPCs expressed markers for committed OPCs (Fig. 5A, C). As a result of performed immunocytochemistry and counted the OPCs of WT iPSCs, 65.79% of A2B5 positive cells, 99.73% of NG2 positive cells, 97.89% of PDGF receptor alpha positive cells, and 92.49% of SOX10 positive cells (Fig. 5B). Two weeks after plating, OPCs were cultured in the presence of 3,3',5'-Triiodo-L-thyronine sodium salt for an additional maintain for 3-4 weeks to achieve terminal differentiation. O4 and Myelin basic protein (MBP), a marker for oligodendrocyte maturity, is usually observed after differentiation (Fig. 5A). During induced OPC differentiation, no difference in the cellular morphology or differentiation ability was observed among the OPCs derived from WT iPSCs, CCALD iPSCs, and AMN iPSCs. When A2B5 positive cells differentiated from WT, CCALD, and AMN iPSC were compared, there was no difference in differentiation into OPCs at 77.05%, 79.80%, and 79.20, respectively (Fig. 5D). These results show that, there was no difference in cell morphology or expressed

oligodendrocyte markers between WT iPSCs and X-ALD iPSCs.

A

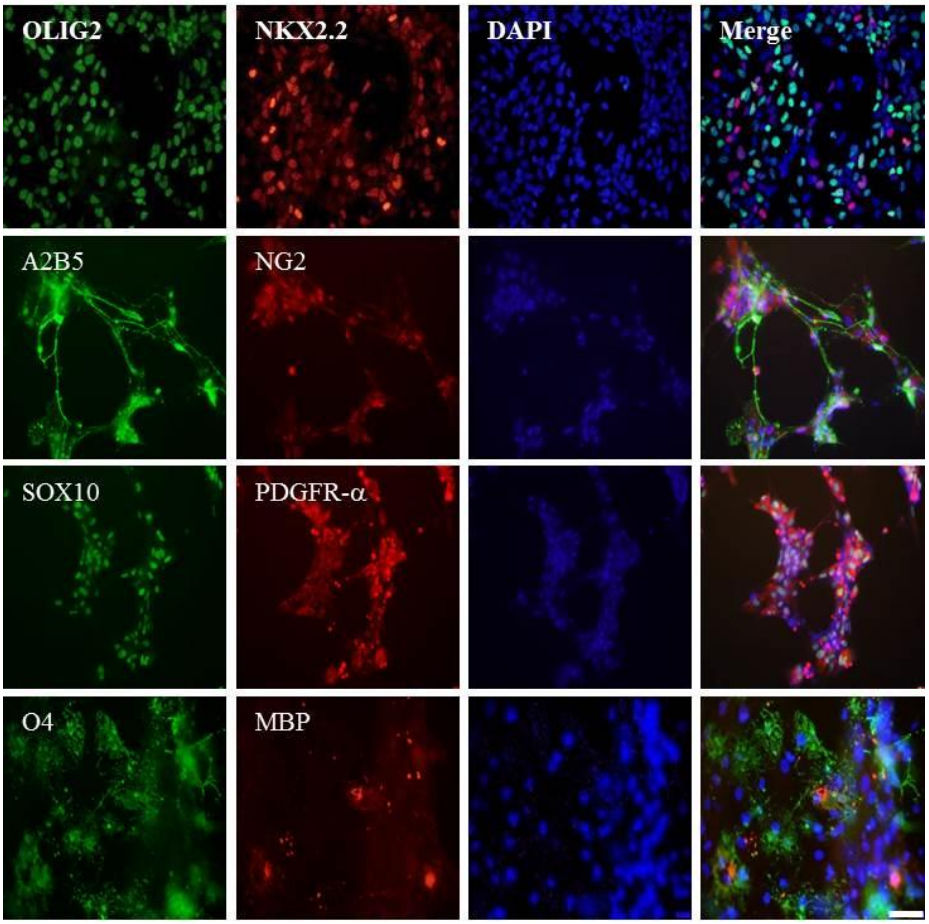

B

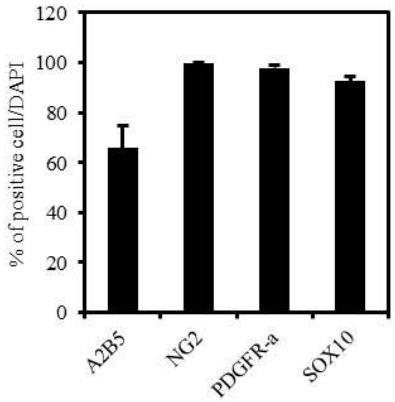

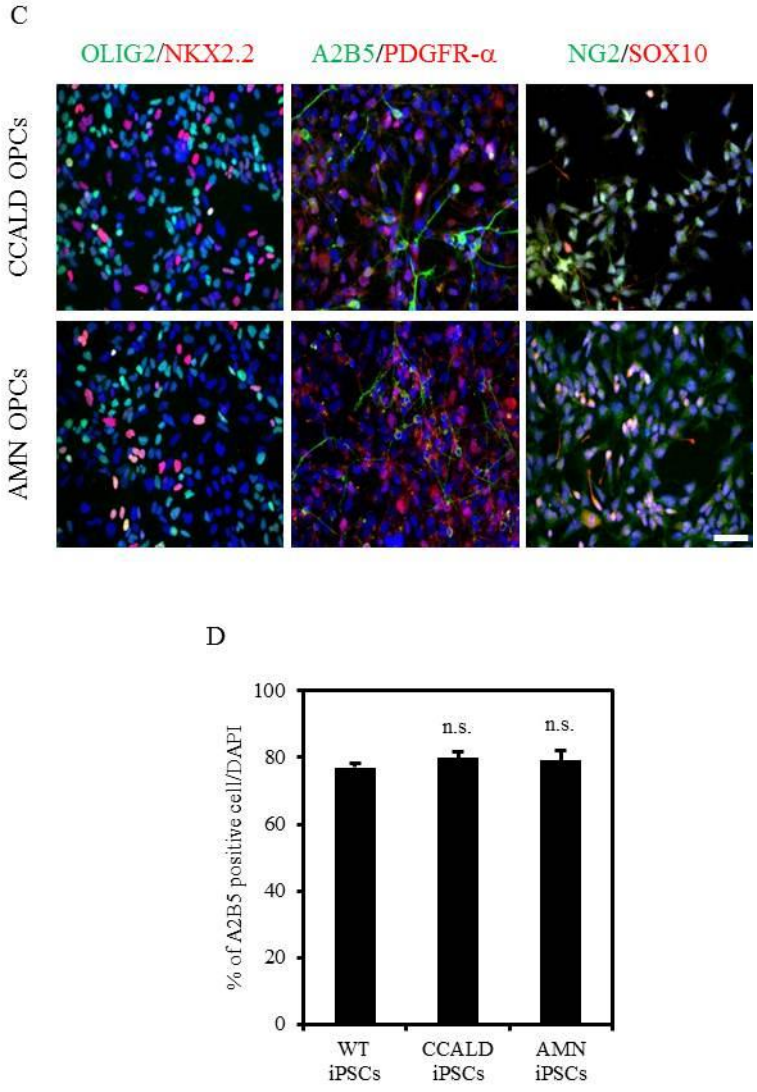

Figure 5. Oligodendrocytes differentiated from X-ALD iPSCs. (A, C) Cells expressing OPC and OL markers positive cells were generated from WT, CCALD, and AMN iPSCs. (B) Quantification of OPC marker positive cells differentiated from WT iPSCs (n = 3). (D) Quantification of A2B5 positive cells were differentiated from WT, CCALD, AMN iPSCs (n = 3). Data is presented as mean ± SEM. A2B5 positive cells were differentiated from CCALD and AMN iPSCs groups were compared with the A2B5 positive cell

differentiated from WT iPSCs group with a two-tailed Student's t-tests. n.s., not significant. Scale bar = 50 μm.

3. Disease modeling of X-ALD iPSCs

Oligodendrocytes were differentiated from X-ALD iPSCs from patient-derived fibroblasts. The oligodendrocytes differentiated from WT, CCALD, and AMN iPSCs did not differ morphologically. However, a sufficient amount of oligodendrocyte cells could not be secured for VLCFAs measurement using GC-MS, and thus VLCFAs were measured only for neurons differentiated from X-ALD (CCALD) and WT iPSCs.

To determine whether neurons differentiated from X-ALD iPSCs had accumulated VLCFA, which is a phenotype of X-ALD, VLCFA levels (C26:0/C22:0 ratio) were measured via GC-MS. VLCFA levels (C26:0/C22:0 ratio) in the neurons of CCALD type was significantly higher than that in their WT neurons, suggesting that X-ALD iPSCs recapitulated and modeled the pathophysiology of X-ALD disease (Fig. 6). These results suggest that the stronger clinical manifestations of CCALD might be associated with abnormal VLCFA accumulation in neurons.

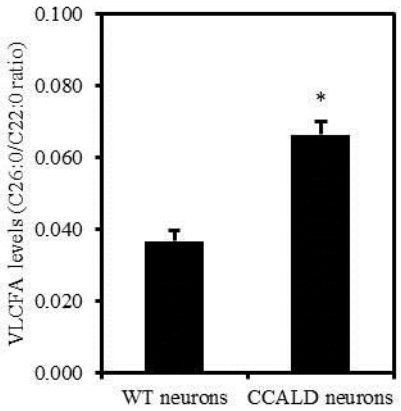

Figure 6. VLCFA levels (C26:0/C22:0 ratio) in neurons derived from X-ALD (CCALD) and WT iPSCs. Data is shown as mean ± SEM. VLCFA levels of the CCALD neurons were compared with those of the WT-neurons, with two-tailed Student's t-tests (n = 3). * $p < 0.05$.

4. *ABCD2* reporter cell lines were established for drug screening

Previously, luciferase reporter constructs were established.[45] The luciferase reporter constructs used in the previous experiment were used for drug screening. The promoter activities of various lengths of *ABCD2* promoters in X-ALD fibroblasts were measured to determine the lengths that maximized transcriptional activity effectiveness. Fragments containing the region of -1300 to -500 bp upstream of the *ABCD2* promoter showed only a 2.3-fold increase in activity compared to the pGL3 basic group. However, the regions that were -1300 bp, -800 bp, and -500 bp upstream of the *ABCD2* promoter fragments showed full transcriptional activity compared to the pGL3 basic group. These results indicate that the region -500 bp upstream of the *ABCD2* promoter is an important region for transcriptional activity. Based on these results, X-ALD iPSC reporter cell lines were also established (Fig. 7).

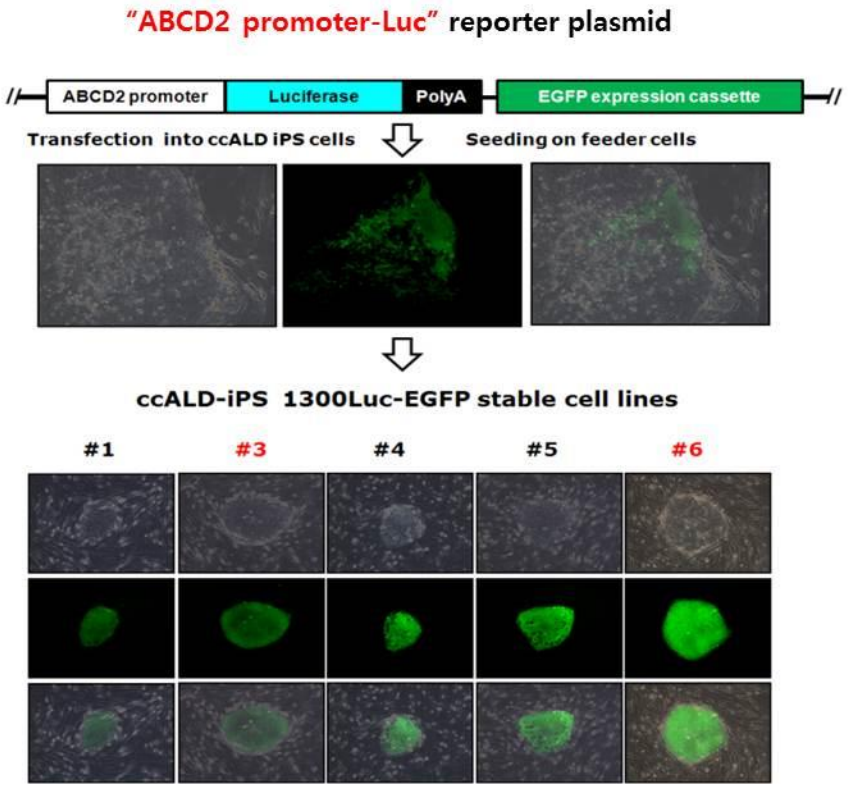

Figure 7. Images of luciferase and GFP reporter cell line established with X-ALD iPSCs. A microporator was used to transfect -1300 bp upstream of the *ABCD2* promoter into CCALD iPSCs.

5. Promoter activity caused by treatment with *ABCD2* gene-inducing drugs

Most small molecules that have been investigated for use as *ABCD2* gene-upregulating agents have been developed by analyzing the promoter region of *ABCD2*. Biological targets of these agents have been limited to transcription factors and epigenetic regulators that can also modify many other off-target proteins. A novel molecule that specifically induces *ABCD2* expression should be discovered to avoid side effects that arise when off-target proteins are affected. A reporter gene assay system was developed using X-ALD fibroblasts to pharmacologically screen active compounds. The regions that were -1300 bp, -800 bp, and -500 bp upstream of the *ABCD2* promoter fragments showed full transcriptional activity. The effects of lovastatin and 4-PBA, which upregulate *ABCD2* gene expression, on luciferase activity were investigated using the -800 bp promoter fragment. Trials with each combination of one and two copies of the *ABCD2* promoter fragments, 1 μM and 4 μM of lovastatin and 1 mM, 4 mM of 4-PBA were conducted. One and two copies of the *ABCD2* promoter fragments engaged in transcriptional activity after treatment with lovastatin and 4-PBA and the trials with two copies exhibited more transcriptional activity than those with one copy, the least of which was a 1.3-fold increase and the greatest of which was a 4.5-fold increase compared to DMSO treatment conditions (Fig. 8). Thus, two copies of the -800 bp promoter region were added to luciferase reporter construct to increase the luciferase signal.

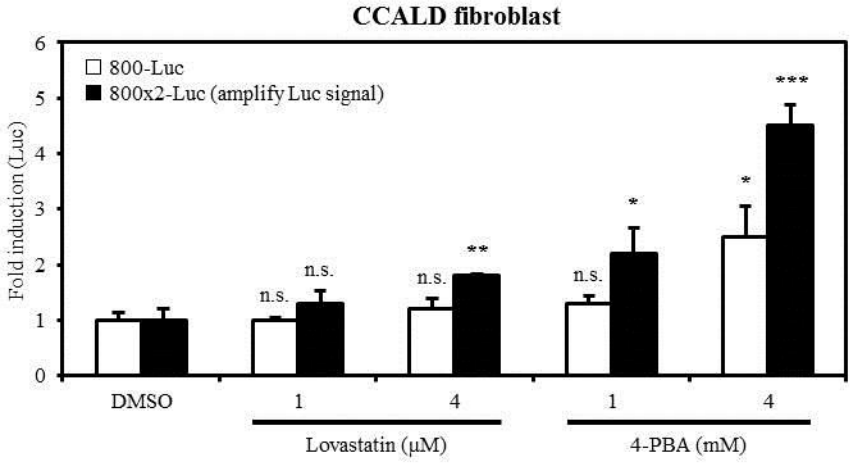

Figure 8. Promoter activity response to treatment with *ABCD2*-inducing drugs. CCALD fibroblasts were transfected with ph*ABCD2* (-800)-Luc or ph*ABCD2* (-800x2)-Luc. Then they were treated with 1 μM, or 4 μM of lovastatin, and 1 mM, or 4 mM of 4-PBA for 3 days. Luciferase activity was measured and normalized by Renilla luciferase activity (n = 3). Data is presented as mean ± SEM. The lovastatin- and 4-PBA-treated groups were compared with the DMSO-treated group using two-tailed Student's t-tests. * $p < 0.05$; ** $p < 0.01$; *** $p < 0.001$; n.s., not significant.

6. Screening of *ABCD2* upregulating compounds

Drug screening was conducted using a LOPAC 1280 library of pharmacologically active compounds (Sigma-Aldrich).

X-ALD fibroblasts were transfected with ph*ABCD2* (-800x2)-Luc and then seeded on 96-well plates Then they were screened by being treated with 10 μM of each of 1,280 pharmacologically active compounds for 1 day. The 64 compounds that increased *ABCD2* expression levels 2.5-fold above that of DMSO were selected for drug screening (Fig. 9). Then X-ALD fibroblasts transfected with ph*ABCD2* (-800x2)-Luc and seeded on 96-well plates were retested with 5 μM of each of these 64 compounds for 3 days. The 9 compounds that showed similar luciferase signals as 1 mM of 4-PBA, which was used as the positive control, were selected for further testing (Fig. 10).

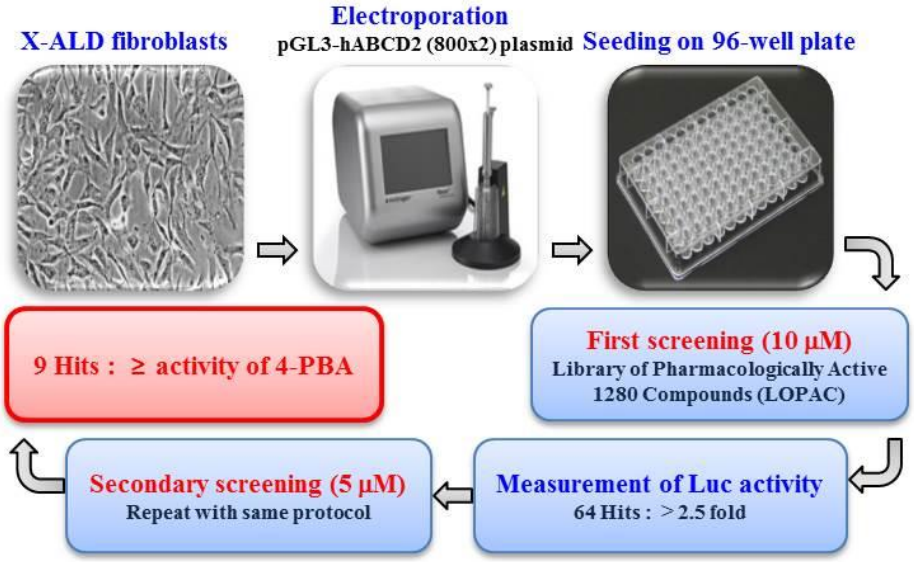

Figure 9. Schematic representation of drug screening procedure. Transfected X-ALD fibroblasts were seeded on 96-well plates. Then a two-step drug screening procedures was performed. The standards for each step were different. Finally, 9 compounds were selected.

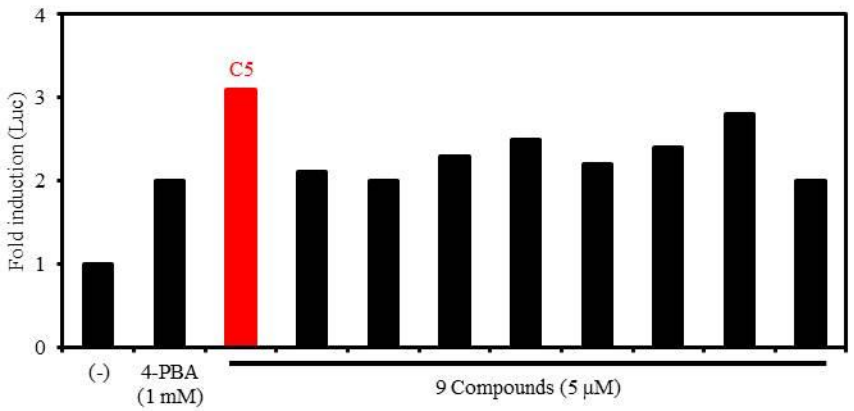

Figure 10. *ABCD2* promoter activity caused by treatment with 9 candidate compounds. Transfected X-ALD fibroblasts were tested with 5 μM each of 64 compounds for 3 days, 9 of which had effects similar to 4-PBA (n = 1). Luciferase activities were measured and normalized by Renilla luciferase activity.

7. *ABCD2* expression and VLCFA levels (C26:0/C22:0 ratio) after candidate compound treatment

CCALD fibroblasts were treated with 3 μM of the 9 selected compounds each for 3 days. *ABCD2* expressed was analyzed by real-time PCR. Although treatment with each of the compounds increased *ABCD2* expression (Fig. 11A), only the C5 compound reduced VLCFA levels (C26:0/C22:0 ratio) without affecting C22:0 levels (Fig. 11B). The A9 compound increased C22:0 levels (Fig. 11C). Therefore, the C5 compound was selected for further investigation.

A

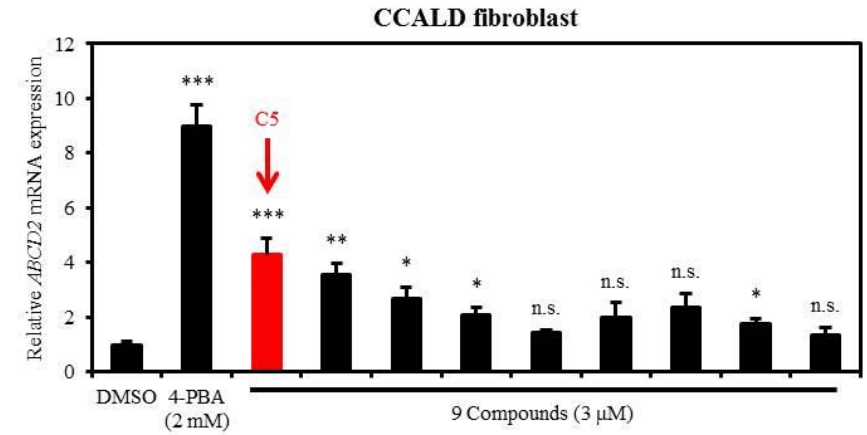

B

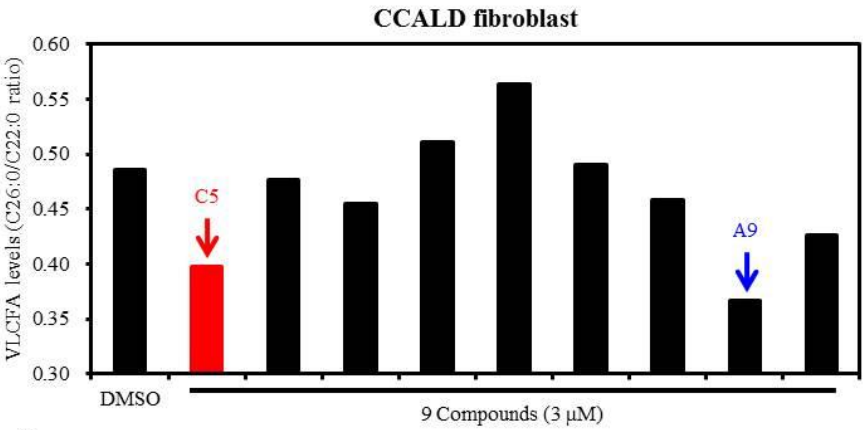

C

	Very Long Chain Fatty Acids				
	C22:0	C24:0	C26:0	C24:0/C22:0	C26:0/C22:0
DMSO	0.837	2.709	0.407	3.237	0.486
C5	0.835	2.363	0.332	2.830	0.398
A9	2.521	6.972	0.924	2.766	0.367

Figure 11. *ABCD2* gene expression and VLCFA levels (C26:0/C22:0 ratio) following treatment by 9 candudate compounds. (A) *ABCD2* gene expression as determined by real-time PCR and normalized to *GAPDH* expression after CCALD fibroblast cells were treated with a total of 3 μM of

each of the selected for 3 days (n = 3). (B) VLCFA levels (C26:0/C22:0 ratio) as determined by GC-MS after CCALD fibroblast cells were treated with a total of 3 μM of each of the 9 selected compounds for 5 days (n = 1). (C) VLCFA levels in fibroblasts treated with C5 and A9 compounds. Data is presented as mean ± SEM. The 4-PBA and the 9 selected compounds were compared with the DMSO treatment group with a two-tailed Student's t-tests. * $p < 0.05$; ** $p < 0.01$; *** $p < 0.001$; n.s., not significant.

8. *ABCD2* gene expression and VLCFA levels (C26:0/C22:0 ratio) by C5 compound dose

CCALD fibroblasts were treated with 3, 6, or 9 μM of commercially available C5 compound for 1, 2, 3, or 5 days. Their *ABCD2* expression levels and VLCFA levels (C26:0/C22:0) were measured by real-time PCR and GC-MS respectively. CCALD fibroblasts were treated with 3 μM or 6 μM C5 compound for 3 days and their *ABCD2* expression levels were compared with those of fibroblasts treated with DMSO or 2 mM of 4-PBA. 4-PBA was used as a positive control for *ABCD2* expression. *ABCD2* expression in C5 compound-treated CCALD fibroblasts was 2.5-fold and 4.7-fold greater than in DMOS-treated CCALD fibroblasts, respectively (Fig. 12A). Those treated with 6 μM of C5 had *ABCD2* expression levels as those treated with 2 mM of 4-PBA. These results indicate that *ABCD2* expression is positively correlated with C5 compound dose.

Similar results were obtained for VLCFA levels (C26:0/C22:0 ratio) as measured by GC-MS. The VLCFA levels (C26:0/22:0 ratio) in the DMSO-treated fibroblasts and the fibroblasts treated with 3, 6, 9 μM of C5 compound for 5 days were 0.52 measured by treating C5 compound with 3 μM, 6 μM, and 9 μM for 5 days, the DMSO-treat, 0.38. 0.32 and 0.17, respectively. Thus, VLCFA levels (C26:0/22:0 ratio) were shown to be negatively correlated with C5 compound dose. Treatment with 2 mM of 4-PBA did not decrease VLCFA levels (C26:0/C22:0 ratio) to 0.57 (Fig. 12B). These results show that C5 compound upregulates *ABCD2* expression and downregulates VLCFA levels (C26:0/C22:0 ratio) in dose-dependent manners.

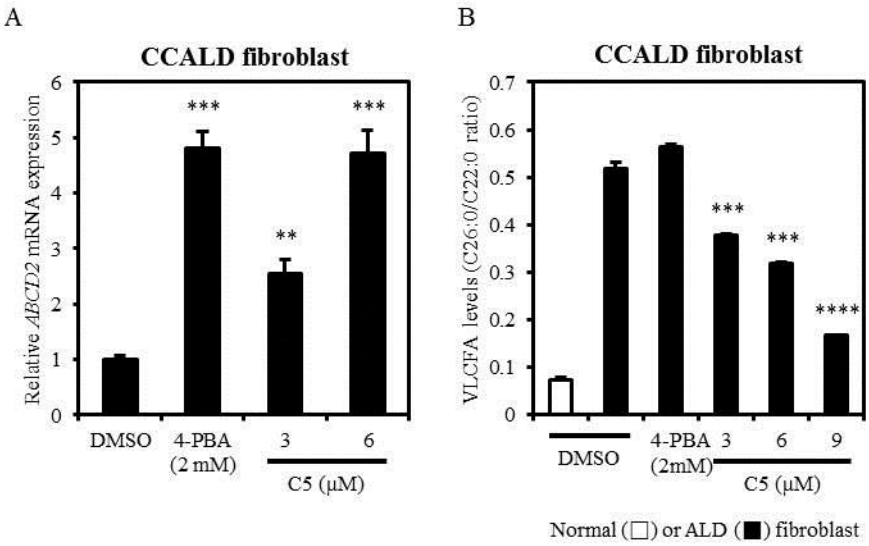

Figure 12. *ABCD2* gene expression and VLCFA levels (C26:0/C22:0 ratio) in CCALD patient-derived fibroblasts after C5 compound treatment by dose. (A) CCALD fibroblast cells were treated with 3 or 6 μM of C5 compound for for 3 days and their *ABCD2* expression was determined by real-time PCR and normalized to *GAPDH* expression (n = 3). (B) CCALD fibroblast cells were treated with 3, 6, or 9 μM of C5 compound for 5 (n = 3). Their VLCFA levels (C26:0/C22:0 ratio) were determined by GC-MS. Data is presented as mean ± SEM. C5 compound-treated groups were compared with the DMSO treatment group with a two-tailed Student's t-tests. * $p < 0.05$; ** $p < 0.01$; *** $p < 0.001$; **** $p < 0.0001$; n.s., not significant.

9. *ABCD2* expression levels and VLCFA levels (C26:0/C22:0 ratio) over time after C5 compound treatment

CCALD fibroblasts were treated with 3 μ of C5 compound for 1, 2, or 3 days and their *ABCD2* expression levels were compared with those of fibroblasts treated with DMSO for the same periods. Their *ABCD2* expression levels and VLCFA levels (C26:0/C22:0) were measured by real-time PCR and GC-MS, respectively. The fibroblasts treated with C5 compound for 1 and 2 days had 1.5-fold and 2.4-fold higher ABCD2 expression levels than DMSO-treated fibroblasts, respectively (Fig. 13A). These results show that *ABCD2* expression increased in a time-dependent manner as a result of C5 compound treatment. The fibroblasts were also treated with 3 μM of C5 compound for 1 day and 3 days. The VLCFA levels (C26:0/C22:0 ratio) of the DMSO-treated fibroblasts and those treated with C5 compound for 1 and 3 days were 0.45, 0.36, and 0.33, respectively, indicating that VLCFA levels (C26:0/C22:0 ratio) decreased in a time-dependent manner as a result of C5 compound treatment (Fig. 13B).

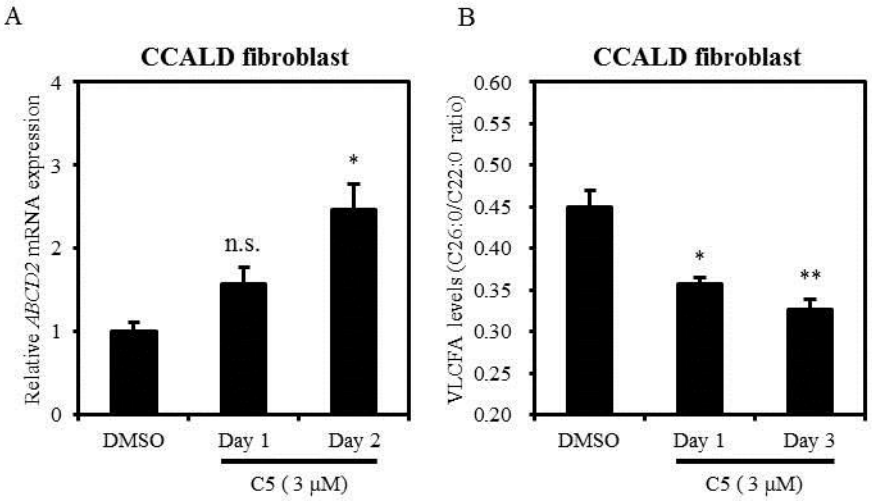

Figure 13. The effect of C5 compound on *ABCD2* expression and VLCFA levels (C26:0/C22:0 ratio) in CCALD patient-derived fibroblasts over time. (A) *ABCD2* expression as determined by real-time PCR and normalized to *GAPDH* expression in CCALD fibroblast cells treated with 3 μM of C5 compound for 1 and 2 days (n = 3). (B) VLCFA levels (C26:0/C22:0 ratio) as determined by GC-MS in CCALD fibroblast cells treated with 3 μM of C5 compound was treated for 1 and 3 days (n = 3). Data is presented as mean ± SEM. The C5 compound-treated groups were compared with the DMSO-treated group using two-tailed Student's t-tests. * $p < 0.05$; ** $p < 0.01$; n.s., not significant.

10. *ABCD2* expression and VLCFA levels (C26:0/C22:0 ratio) in AMN patient-derived fibroblasts treated with C5 compound

AMN-type fibroblasts were also treated with C5 compound. *ABCD2* expression was 6.9-fold and 10.3-fold higher in fibroblasts treated with 3 and 6 μM of C5 compound, respectively, than in compared to DMSO-treated fibroblasts (Fig. 14A). VLCFA levels (C26:0/C22:0 ratio) in the DMSO-treated fibroblasts were 0.22 while those in fibroblasts treated with 3, 6, 9 μM of C5 compound were 0.16, 0.15 and 0.14, (Fig. 14B).

These results showed that the C5 compound upregulates *ABCD2* gene expression and downregulates VLCFA levels in AMN-type fibroblasts.

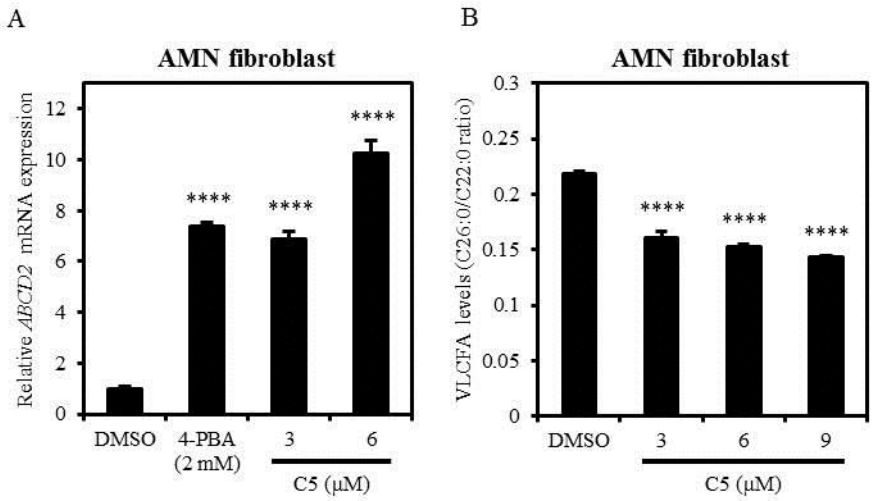

Figure 14. *ABCD2* expression and VLCFA levels (C26:0/C22:0 ratio) in AMN patient-derived fibroblasts treated with C5 compound. (A) AMN fibroblast cells were treated with 3 or 6 μM of C5 compound for 3 days and their *ABCD2* expression levels were analyzed by real-time PCR and normalized to *GAPDH* expression (n = 3). (B) AMN fibroblast cells were treated with 3, 6, or 9 μM of C5 compound for 3 days and their VLCFA levels (C26:0/C22:0 ratio) were determined by GC-MS (n = 3). Data is presented as mean ± SEM. The C5 compound-treated groups were compared with the DMSO-treated group using two-tailed Student's t-tests. * $p < 0.05$; ** $p < 0.01$; *** $p < 0.001$; **** $p < 0.0001$; n.s., not significant.

11. C5 compound toxicity in CCALD fibroblasts

In vitro cytotoxicity testing provides crucial safety information. 3-(4, 5-dimethylthiazol-2-yl)-2,5-diphenyltetrazolium bromide (MTT) assays were conducted to measure cellular metabolic activity as an indicator of cell viability, proliferation and cytotoxicity. This colorimetric assay is based on the reduction of a yellow tetrazolium salt (MTT) to purple formazan crystals by metabolically active cells. [47,48]

CCALD fibroblasts were treated with 1, 3, and 6 μM of C5 compound for 1, 2, or 3 days and their O.D. values were compared with those of DMSO-treated fibroblasts. There were no statistically significant differences between the groups (Fig. 15). This result shows that the C5 compound was non-toxic under these experimental conditions.

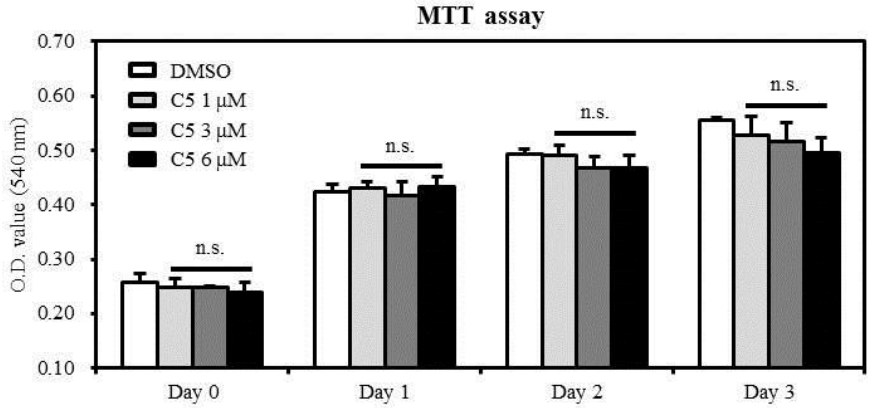

Figure 15. C5 compound toxicity in CCALD fibroblasts. CCALD fibroblasts were treated with 1, 3, or 6 μM of C5 compound for 1, 2, or 3 days and then MTT assays were performed. Data is presented as mean ± SEM. The C5 compound-treated groups were compared with the DMSO-treated group using two-tailed Student's t-tests. n.s., not significant.

IV. Discussion

Increased VLCFAs are the biochemical signature of X-ALD and cause its pathogenesis.[46] The overexpression of *ABCD2* has been hypothesized to be a potential therapeutic target for *ABCD1* deficiency in X-ALD patients.[49] Many drugs have been tested for their ability to reduce VLCFA levels by upregulating *ABCD2* expression, but they also reduced VLCFA levels outside of a limited range, such as patient-derived fibroblast cells, X-ALD animal models, and patient blood.

Currently, only Lorenzo's oil is administered to ALD patients. Lorenzo's oil lowers elevated VLCFA levels in the blood of symptomatic patients[50] and may prevent the onset of CCALD but it does not stop inflammation as a result of demyelination in cerebral white matter.[51] Lorenzo's oil does not lower VLCFA levels in the brain because of its low active concentration and so is rapidly metabolized in the brain.[52] Lorenzo's oil reduces VLCFA levels by competitively inhibiting the ELOVL1 enzyme, which is involved in the rate-limiting step.[53] Recently, sobetirome, a clinical-stage selective thyroid hormone receptor agonist, was show to increase cerebral *ABCD2* expression and lower VLCFA levels in the blood, peripheral organs, and brains of mice with defective *ABCD1*.[29] It is more desirable to induce *ABCD2* expression in tissue affected by X-ALD, namely adrenal tissue, the testes, and the brain, and specific cell types, such as oligodendrocytes.

In this study, iPSCs were generated from an X-ALD patient's cells and the accumulation of VLCFAs was confirmed by differentiating iPSCs into neurons and oligodenrocytes. Drug screening was conducted by transfecting CCALD fibroblasts with two copies of -800-Luc reporter plasmids containing the *ABCD2* gene promoter region. C5 compound was identified from among 1,280 bioactive small molecules as being able to lower VLCFA levels by *ABCD2* expression.

C5 compound is the derivative of amiloride, the Na+/H+ exchanger

(NHE) inhibitor, and other derivatives include EIPA, cariporide, and DMA. Both C5 compound and EIPA have similar selectivity profiles, which are NHE1 > NHE2 > NHE5 > NHE3.[54] Cariporide is more NHE1-selective inhibitor than C5 compound and inactive on NHE3 and NHE5. DMA is less potent as an NHE inhibitor than C5 compound and it has not been reported to inhibit activity on NHE5. Although it is possible that C5 compound reduced VLCFA levels via another mechanism, this study was conducted with NHE inhibition as the therapeutic target for treating X-ALD.

NHE is involved in the intracellular pH homeostasis of many mammalian cell types. NHE isoforms share 20-60% of their amino acid identities and are distributed in various tissues.[55] Given that X-ALD fibroblasts responded to C5 compound treatment, it can be inferred that NHE is expressed in X-ALD fibroblasts, so by knocking-down the expressed NHE subtype would indicate which NHE subtype upregulates *ABCD2* expression. This information would indicate how NHE mediates *ABCD2* expression induction.

Most amiloride derivatives and other related chemicals were developed to target NHE1 and there are no other known NHE subtype-specific amiloride derivatives available. C5 compound and EIPA have the most potent inhibitory activity against NHE5.[54] Troglitazone is believed to inhibit NHE1 indirectly by activating ERK. This hypothesis also indicates that NHE5 inhibition may not be related to *ABCD2* expression induction. NHE5 is a direct target for phosphorylation by AMPK, a key regulator of cellular energy homeostasis. NHE5 activity is regulated by the AMPK, the AICAR and AMPK inhibitors, and Compound C.[56] This AMPK will also provide clues C5 compound's mechanism and indicate candidates for ALD treatment. A recent report showed that AMPK activator metformin increases *ABCD2* expression and reduces VLCFA levels in X-ALD fibroblast.[30]

In this study, C5 compound was shown to induce *ABCD2* expression in X-ALD fibroblasts. NHE inhibition selectively induces *ABCD2* expression.

NHE5's most distinguishing characteristic is the fact that it is almost exclusively expressed in the central nervous system.[57] Like its closest homologue NHE3, NHE5 is located at both the plasma membrane and recycling endosomes. NHE5 negatively regulates dendritic spine growth.[58] NHE5 overexpression blocks dendritic spine growth in response to neuronal activity. NHE5-deficient mice exhibit markedly better learning and memory than those with normal amounts of NHE5, indicating that NHE5 could a candidate therapeutic target for improving cognition.[59] p-CaMKII and p-ERK1/2 levels are higher in $NHE^{-/-}$ brain tissue than in other tissue, which may activate CREB phosphorylation. p-CaMKII and p-ERK1/2 increase fatty acid uptake and oxidation.[60] Acute muscle contraction or exercise initiate the most important signaling cascades in fatty acid uptake and oxidation regulation, such as AMPK, CaMKII, and ERK1/2.[61] The inhibition or knock-out of specific NHE subtypes may trigger similar signal cascades and upregulate fatty acid oxidation, which requires more energy sources, such as VLCFAs. However the relationship between NHE and the upregulation of *ABCD2* expression needs to be further investigated. This study's results showed the novel result that upregulating *ABCD2* expression limits NHE inhibition, which dwonregulates VLCFA. Specific NHE subtype inhibitors or extracellular antibodies may be a safer potential X-ALD therapy.

V. Conclusion

Human hiPSCs serve as a powerful disease modeling platform. Disease modeling can be used to understand disease mechanisms and to screen for drugs that can be used against them. Understanding disease and drug-screening mechanism can help identify treatments for currently incurable diseases. There is currently no cure for X-ALD, but efforts are being made to find. X-ALD is caused by the *ABCD1* mutation, which causes VLCFAs to accumulate in the body. In order to solve this problem, various efforts have been made to increase the expression of *ABCD2*, which is a homologue of *ABCD1*. In this study, C5 compound was identified by luciferase reporter-based high-throughput screening and was shown to increase *ABCD2* expression in a time- and dose-dependent manner and thus decreased VLCFA levels. This result shows that it is a potential therapeutic agent for treating X-ALD.

References

1. Thomas JH. Thinking about genetic redundancy. Trends Genet 1993;9:395-9.
2. Gu Z, Steinmetz LM, Gu X, Scharfe C, Davis RW, Li WH. Role of duplicate genes in genetic robustness against null mutations. Nature 2003;421:63-6.
3. Passegue E, Jochum W, Behrens A, Ricci R, Wagner EF. JunB can substitute for Jun in mouse development and cell proliferation. Nat Genet 2002;30:158-66.
4. Maconochie M, Nonchev S, Morrison A, Krumlauf R. Paralogous Hox genes: function and regulation. Annu Rev Genet 1996;30:529-56.
5. Hoffmann FM. Drosophila abl and genetic redundancy in signal transduction. Trends Genet 1991;7:351-5.
6. Normanly J, Bartel B. Redundancy as a way of life - IAA metabolism. Curr Opin Plant Biol 1999;2:207-13.
7. Dubois-Dalcq M, Feigenbaum V, Aubourg P. The neurobiology of X-linked adrenoleukodystrophy, a demyelinating peroxisomal disorder. Trends Neurosci 1999;22:4-12.
8. Moser HW, Loes DJ, Melhem ER, Raymond GV, Bezman L, Cox CS, et al. X-Linked adrenoleukodystrophy: overview and prognosis as a function of age and brain magnetic resonance imaging abnormality. A study involving 372 patients. Neuropediatrics 2000;31:227-39.
9. Singh I, Moser AE, Moser HW, Kishimoto Y. Adrenoleukodystrophy: impaired oxidation of very long chain fatty acids in white blood cells, cultured skin fibroblasts, and amniocytes. Pediatr Res 1984;18:286-90.
10. Powers JM. Adreno-leukodystrophy (adreno-testiculo-leukomyelo-neuropathic-complex). Clin Neuropathol 1985;4:181-99.
11. Bezman L, Moser AB, Raymond GV, Rinaldo P, Watkins PA, Smith KD, et al. Adrenoleukodystrophy: incidence, new mutation rate, and results of extended family screening. Ann Neurol 2001;49:512-7.
12. Moser HW, Mahmood A, Raymond GV. X-linked adrenoleukodystrophy. Nat Clin Pract Neurol 2007;3:140-51.
13. Dubey P, Raymond GV, Moser AB, Kharkar S, Bezman L, Moser HW. Adrenal insufficiency in asymptomatic adrenoleukodystrophy patients identified by very long-chain fatty acid screening. J Pediatr 2005;146:528-32.
14. Kemp S, Wei HM, Lu JF, Braiterman LT, McGuinness MC, Moser AB, et al. Gene redundancy and pharmacological gene therapy: implications for X-linked adrenoleukodystrophy. Nat Med 1998;4:1261-8.

15. Netik A, Forss-Petter S, Holzinger A, Molzer B, Unterrainer G, Berger J. Adrenoleukodystrophy-related protein can compensate functionally for adrenoleukodystrophy protein deficiency (X-ALD): implications for therapy. Hum Mol Genet 1999;8:907-13.
16. Pujol A, Ferrer I, Camps C, Metzger E, Hindelang C, Callizot N, et al. Functional overlap between ABCD1 (ALD) and ABCD2 (ALDR) transporters: a therapeutic target for X-adrenoleukodystrophy. Hum Mol Genet 2004;13:2997-3006.
17. Lombard-Platet G, Savary S, Sarde CO, Mandel JL, Chimini G. A close relative of the adrenoleukodystrophy (ALD) gene codes for a peroxisomal protein with a specific expression pattern. Proc Natl Acad Sci U S A 1996;93:1265-9.
18. Troffer-Charlier N, Doerflinger N, Metzger E, Fouquet F, Mandel JL, Aubourg P. Mirror expression of adrenoleukodystrophy and adrenoleukodystrophy related genes in mouse tissues and human cell lines. Eur J Cell Biol 1998;75:254-64.
19. Gondcaille C, Depreter M, Fourcade S, Lecca MR, Leclercq S, Martin PG, et al. Phenylbutyrate up-regulates the adrenoleukodystrophy-related gene as a nonclassical peroxisome proliferator. J Cell Biol 2005;169:93-104.
20. Fourcade S, Ruiz M, Guilera C, Hahnen E, Brichta L, Naudi A, et al. Valproic acid induces antioxidant effects in X-linked adrenoleukodystrophy. Hum Mol Genet 2010;19:2005-14.
21. Singh J, Khan M, Singh I. HDAC inhibitor SAHA normalizes the levels of VLCFAs in human skin fibroblasts from X-ALD patients and downregulates the expression of proinflammatory cytokines in Abcd1/2-silenced mouse astrocytes. J Lipid Res 2011;52:2056-69.
22. Singh J, Khan M, Singh I. Caffeic acid phenethyl ester induces adrenoleukodystrophy (Abcd2) gene in human X-ALD fibroblasts and inhibits the proinflammatory response in Abcd1/2 silenced mouse primary astrocytes. Biochim Biophys Acta 2013;1831:747-58.
23. Weinhofer I, Forss-Petter S, Zigman M, Berger J. Cholesterol regulates ABCD2 expression: implications for the therapy of X-linked adrenoleukodystrophy. Hum Mol Genet 2002;11:2701-8.
24. Berger J, Albet S, Bentejac M, Netik A, Holzinger A, Roscher AA, et al. The four murine peroxisomal ABC-transporter genes differ in constitutive, inducible and developmental expression. Eur J Biochem 1999;265:719-27.
25. Fourcade S, Savary S, Albet S, Gauthe D, Gondcaille C, Pineau T, et al. Fibrate induction of the adrenoleukodystrophy-related gene (ABCD2): promoter analysis and role of the peroxisome proliferator-activated receptor PPARalpha. Eur J Biochem 2001;268:3490-500.
26. Gondcaille C, Genin EC, Lopez TE, Dias AM, Geillon F, Andreoletti

P, et al. LXR antagonists induce ABCD2 expression. Biochim Biophys Acta 2014;1841:259-66.
27. Fourcade S, Savary S, Gondcaille C, Berger J, Netik A, Cadepond F, et al. Thyroid hormone induction of the adrenoleukodystrophy-related gene (ABCD2). Mol Pharmacol 2003;63:1296-303.
28. Genin EC, Gondcaille C, Trompier D, Savary S. Induction of the adrenoleukodystrophy-related gene (ABCD2) by thyromimetics. J Steroid Biochem Mol Biol 2009;116:37-43.
29. Hartley MD, Kirkemo LL, Banerji T, Scanlan TS. A Thyroid Hormone-Based Strategy for Correcting the Biochemical Abnormality in X-Linked Adrenoleukodystrophy. Endocrinology 2017;158:1328-38.
30. Singh J, Olle B, Suhail H, Felicella MM, Giri S. Metformin-induced mitochondrial function and ABCD2 up-regulation in X-linked adrenoleukodystrophy involves AMP-activated protein kinase. J Neurochem 2016;138:86-100.
31. Stumpf DA, Hayward A, Haas R, Frost M, Schaumburg HH. Adrenoleukodystrophy. Failure of immunosuppression to prevent neurological progression. Arch Neurol 1981;38:48-9.
32. Korenke GC, Christen HJ, Kruse B, Hunneman DH, Hanefeld F. Progression of X-linked adrenoleukodystrophy under interferon-beta therapy. J Inherit Metab Dis 1997;20:59-66.
33. Berger J, Pujol A, Aubourg P, Forss-Petter S. Current and future pharmacological treatment strategies in X-linked adrenoleukodystrophy. Brain Pathol 2010;20:845-56.
34. Cappa M, Bertini E, del Balzo P, Cambiaso P, Di Biase A, Salvati S. High dose immunoglobulin IV treatment in adrenoleukodystrophy. J Neurol Neurosurg Psychiatry 1994;57 Suppl:69-70; discussion 1.
35. Jonch AE, Danielsen ER, Thomsen C, Meden P, Svenstrup K, Nielsen JE. Intravenous immunoglobulin treatment in a patient with adrenomyeloneuropathy. BMC Neurol 2012;12:108.
36. Eichler F, Duncan C, Musolino PL, Orchard PJ, De Oliveira S, Thrasher AJ, et al. Hematopoietic Stem-Cell Gene Therapy for Cerebral Adrenoleukodystrophy. N Engl J Med 2017;377:1630-8.
37. Takahashi K, Tanabe K, Ohnuki M, Narita M, Ichisaka T, Tomoda K, et al. Induction of pluripotent stem cells from adult human fibroblasts by defined factors. Cell 2007;131:861-72.
38. Takahashi K, Yamanaka S. Induced pluripotent stem cells in medicine and biology. Development 2013;140:2457-61.
39. Park CY, Kim J, Kweon J, Son JS, Lee JS, Yoo JE, et al. Targeted inversion and reversion of the blood coagulation factor 8 gene in human iPS cells using TALENs. Proc Natl Acad Sci U S A 2014;111:9253-8.
40. Jang J, Yoo JE, Lee JA, Lee DR, Kim JY, Huh YJ, et al.

Disease-specific induced pluripotent stem cells: a platform for human disease modeling and drug discovery. Exp Mol Med 2012;44:202-13.

41. Kang SM, Cho MS, Seo H, Yoon CJ, Oh SK, Choi YM, et al. Efficient induction of oligodendrocytes from human embryonic stem cells. Stem Cells 2007;25:419-24.
42. Kim DS, Lee JS, Leem JW, Huh YJ, Kim JY, Kim HS, et al. Robust enhancement of neural differentiation from human ES and iPS cells regardless of their innate difference in differentiation propensity. Stem Cell Rev Rep 2010;6:270-81.
43. Park CY, Kim HS, Jang J, Lee H, Lee JS, Yoo JE, et al. ABCD2 is a direct target of beta-catenin and TCF-4: implications for X-linked adrenoleukodystrophy therapy. PLoS One 2013;8:e56242.
44. Kim JY, Lee JS, Hwang HS, Lee DR, Park CY, Jung SJ, et al. Wnt signal activation induces midbrain specification through direct binding of the beta-catenin/TCF4 complex to the EN1 promoter in human pluripotent stem cells. Exp Mol Med 2018;50:1-13.
45. Park CY, Kim HS, Jang J, Lee H, Lee JS, Yoo JE, et al. ABCD2 is a direct target of β-catenin and TCF-4: implications for X-linked adrenoleukodystrophy therapy. PLoS One 2013;8:e56242.
46. Moser HW, Moser AB, Kawamura N, Murphy J, Suzuki K, Schaumburg H, et al. Adrenoleukodystrophy: elevated C26 fatty acid in cultured skin fibroblasts. Ann Neurol 1980;7:542-9.
47. Vistica DT, Skehan P, Scudiero D, Monks A, Pittman A, Boyd MR. Tetrazolium-based assays for cellular viability: a critical examination of selected parameters affecting formazan production. Cancer Res 1991;51:2515-20.
48. Berridge MV, Tan AS. Characterization of the cellular reduction of 3-(4,5-dimethylthiazol-2-yl)-2,5-diphenyltetrazolium bromide (MTT): subcellular localization, substrate dependence, and involvement of mitochondrial electron transport in MTT reduction. Arch Biochem Biophys 1993;303:474-82.
49. Berger J, Forss-Petter S, Eichler FS. Pathophysiology of X-linked adrenoleukodystrophy. Biochimie 2014;98:135-42.
50. Aubourg P, Adamsbaum C, Lavallard-Rousseau M-C, Rocchiccioli F, Cartier N, Jambaque I, et al. A Two-Year Trial of Oleic and Erucic Acids ("Lorenzo's Oil") as Treatment for Adrenomyeloneuropathy. New England Journal of Medicine 1993;329:745-52.
51. Moser HW, Raymond GV, Lu SE, Muenz LR, Moser AB, Xu J, et al. Follow-up of 89 asymptomatic patients with adrenoleukodystrophy treated with Lorenzo's oil. Arch Neurol 2005;62:1073-80.
52. Golovko MY, Murphy EJ. Uptake and metabolism of plasma-derived erucic acid by rat brain. J Lipid Res 2006;47:1289-97.
53. Sassa T, Wakashima T, Ohno Y, Kihara A. Lorenzo's oil inhibits ELOVL1 and lowers the level of sphingomyelin with a saturated very

long-chain fatty acid. J Lipid Res 2014;55:524-30.
54. Masereel B, Pochet L, Laeckmann D. An overview of inhibitors of Na(+)/H(+) exchanger. Eur J Med Chem 2003;38:547-54.
55. Alexander RT, Grinstein S. Na+/H+ exchangers and the regulation of volume. Acta Physiol (Oxf) 2006;187:159-67.
56. Jinadasa T, Szabo EZ, Numat M, Orlowski J. Activation of AMP-activated protein kinase regulates hippocampal neuronal pH by recruiting Na(+)/H(+) exchanger NHE5 to the cell surface. J Biol Chem 2014;289:20879-97.
57. Szaszi K, Paulsen A, Szabo EZ, Numata M, Grinstein S, Orlowski J. Clathrin-mediated endocytosis and recycling of the neuron-specific Na+/H+ exchanger NHE5 isoform. Regulation by phosphatidylinositol 3'-kinase and the actin cytoskeleton. J Biol Chem 2002;277:42623-32.
58. Diering GH, Mills F, Bamji SX, Numata M. Regulation of dendritic spine growth through activity-dependent recruitment of the brain-enriched Na(+)/H(+) exchanger NHE5. Mol Biol Cell 2011;22:2246-57.
59. Chen X, Wang X, Tang L, Wang J, Shen C, Liu J, et al. Nhe5 deficiency enhances learning and memory via upregulating Bdnf/TrkB signaling in mice. Am J Med Genet B Neuropsychiatr Genet 2017;174:828-38.
60. Raney MA, Turcotte LP. Evidence for the involvement of CaMKII and AMPK in Ca2+-dependent signaling pathways regulating FA uptake and oxidation in contracting rodent muscle. J Appl Physiol (1985) 2008;104:1366-73.
61. Turcotte LP, Abbott MJ. Contraction-induced signaling: evidence of convergent cascades in the regulation of muscle fatty acid metabolism. Can J Physiol Pharmacol 2012;90:1419-33.

Abstract (in Korean)

환자 유래 역분화 줄기세포를 이용한 X-연관 부신백질이영양증의 질병 모델링 및 약물 스크리닝

<지도교수 김 동 욱>

연세대학교 대학원 의과학과

이 재 석

X-연관 부신백질이영양증 (X-linked adrenoleukodystrophy, X-ALD)은 X 염색체의 ATP-binding cassette subfamily D member 1 (*ABCD1*) 유전자의 돌연변이로 인하여 과산화소체 (peroxisome) 막에 존재하는 수송체인 부신백질이영양증 단백질 (adrenoleukodystrophy protein, ALDP)의 기능 상실로 인해 발생하는 신경퇴행성 질환으로, 장기 및 혈청에 매우 긴사슬 지방산 (very long chain fatty acids, VLCFAs)이 축적된다. 현재 X-연관 부신백질이영양증에 대한 치료 가능한 약물은 없는 실정이다. 로렌조 오일은 뇌 자기공명영상이 정상인 무증상 소년에게 투여 시 매우 긴사슬 지방산의 생성을 억제함으로써 예방 효과가 있는 것으로 알려져 있으나, 이는 질병의 진행속도만을 늦출 뿐, 치료제로서의 역할은 하지 못하고 있다. 과산화소체 막에는 *ABCD1* 이외에 *ABCD2, ABCD3, ABCD4* 유전자가 발현하고 있다. *ABCD2* 유전자는 *ABCD1* 유전자와 가장 비슷한

유전자 서열을 가지고 있으며 기능적으로 중복성을 보인다. 따라서 *ABCD2* 유전자의 과발현을 유도시키는 것은 X-연관 부신백질이영양증에 결함 있는 *ABCD1* 유전자의 대체제로 언급되고 있다. 실제로 *ABCD2* 유전자의 과발현을 유도하기 위한 연구를 해오고 있지만 효과적인 약물은 아직까지 밝혀지지 않았다. 본 연구에서는 질병 모델링 및 신약 개발을 위해, X-연관 부신백질이영양증 환자 유래 섬유아세포를 이용하여 X-연관 부신백질이영양증 역분화 줄기세포 (induced pluripotent stem cell, iPSC)를 생성하고 약물 스크리닝 시스템을 정립하였다. X-연관 부신백질이영양증 역분화 줄기세포는 X-연관 부신백질이영양증의 병태생리학을 모사하고 있어 질병의 모델화가 가능하였다. 또한, luciferase 리포터 기반의 고효율 스크리닝 시스템을 사용하여 약물 스크리닝을 한 결과, X-연관 부신백질이영양증 환자의 섬유아세포에서 *ABCD2* 유전자의 프로모터 활성을 상향 조절하는 X-연관 부신백질이영양증 치료제 후보물질인 C5 화합물을 발굴하였다. C5 화합물은 X-연관 부신백질이영양증 환자 유래 세포에서 용량 및 시간 의존적으로 VLCFA를 감소시켰다. 이 연구의 결과는 C5 화합물이 X-연관 부신백질이영양증에 대한 치료제로서의 잠재성을 가지고 있음을 보여준다.

핵심되는 말: 인간 역분화 줄기세포, X-연관 부신백질이영양증, *ABCD1*, *ABCD2*, 매우 긴사슬 지방산

Publication List

1. Kim JY*****, **Lee JS***, Hwang HS, Lee DR, Park CY, Jung SJ, et al. Wnt signal activation induces midbrain specification through direct binding of the beta-catenin/TCF4 complex to the EN1 promoter in human pluripotent stem cells. Exp Mol Med 2018;50:1-13. (***** co-first author)

2. Kim DS, Jung SJ, **Lee JS**, Lim BY, Kim HA, Yoo JE, et al. Rapid generation of OPC-like cells from human pluripotent stem cells for treating spinal cord injury. Exp Mol Med 2017;49:e361.

3. Park CY, Halevy T, Lee DR, Sung JJ, **Lee JS**, Yanuka O, et al. Reversion of FMR1 Methylation and Silencing by Editing the Triplet Repeats in Fragile X iPSC-Derived Neurons. Cell Rep 2015;13:234-41.

4. Lee DR, Yoo JE, **Lee JS**, Park S, Lee J, Park CY, et al. PSA-NCAM-negative neural crest cells emerging during neural induction of pluripotent stem cells cause mesodermal tumors and unwanted grafts. Stem Cell Reports 2015;4:821-34.

5. Park CY, Kim J, Kweon J, Son JS, **Lee JS**, Yoo JE, et al. Targeted inversion and reversion of the blood coagulation factor 8 gene in human iPS cells using TALENs. Proc Natl Acad Sci U S A 2014;111:9253-8.

6. Park CY, Kim HS, Jang J, Lee H, **Lee JS**, Yoo JE, et al. ABCD2 is a direct target of β-catenin and TCF-4: implications for X-linked adrenoleukodystrophy therapy. PLoS One 2013;8:e56242.

7. Kim DS, **Lee JS**, Leem JW, Huh YJ, Kim JY, Kim HS, et al. Robust enhancement of neural differentiation from human ES and iPS cells regardless of their innate difference in differentiation propensity. Stem Cell Rev Rep 2010;6:270-81.

8. Kim DS, Jung SJ, Nam TS, Jeon YH, Lee DR, **Lee JS**, et al. Transplantation of GABAergic neurons from ESCs attenuates tactile hypersensitivity following spinal cord injury. Stem Cells 2010;28:2099-108.

9. Seo DR, Kim SY, Kim KY, Lee HG, Moon JH, **Lee JS**, et al. Cross talk between P2 purinergic receptors modulates extracellular ATP-mediated interleukin-10 production in rat microglial cells. Exp Mol Med 2008;40:19-26.